

'Trapped rainbow' storage of light in metamaterials

Kosmas L. Tsakmakidis¹, Allan D. Boardman² & Ortwin Hess¹

Light usually propagates inside transparent materials in well known ways¹. However, recent research^{2–6} has examined the possibility of modifying the way the light travels by taking a normal transparent dielectric and inserting tiny metallic inclusions of various shapes and arrangements. As light passes through these structures, oscillating electric currents are set up that generate electromagnetic field moments; these can lead to dramatic effects on the light propagation, such as negative refraction. Possible applications include lenses that break traditional diffraction limits^{3,4} and 'invisibility cloaks' (refs 5, 6). Significantly less research has focused on the potential of such structures for slowing, trapping and releasing light signals. Here we demonstrate theoretically that an axially varying heterostructure with a metamaterial core of negative refractive index can be used to efficiently and coherently bring light to a complete standstill. In contrast to previous approaches for decelerating and storing light^{7–13}, the present scheme simultaneously allows for high in-coupling efficiencies and broadband, room-temperature operation. Surprisingly, our analysis reveals a critical point at which the effective thickness of the waveguide is reduced to zero, preventing the light wave from propagating further. At this point, the light ray is permanently

trapped, its trajectory forming a double light-cone that we call an 'optical clepsydra'. Each frequency component of the wave packet is stopped at a different guide thickness, leading to the spatial separation of its spectrum and the formation of a 'trapped rainbow'. Our results bridge the gap between two important contemporary realms of science—metamaterials and slow light. Combined investigations may lead to applications in optical data processing and storage or the realization of quantum optical memories.

For decades scientists maintained that¹⁴ "optical data cannot be stored statically and must be processed and switched on the fly". The reason for this conclusion was that stopping and storing an optical signal by dramatically reducing the speed of light itself was thought to be infeasible. Undeniably, the absence of any form of interaction between photons and other elementary particles, as well as their enormous speed, makes it excessively difficult to confine them to a finite volume by reducing their velocity down to zero. However, in recent years a series of discoveries contributed towards annulling such assertions and proved conclusively that it is, indeed, possible to bring light to a complete standstill. Amongst others, electromagnetically induced transparency⁷, quantum-dot semiconductor

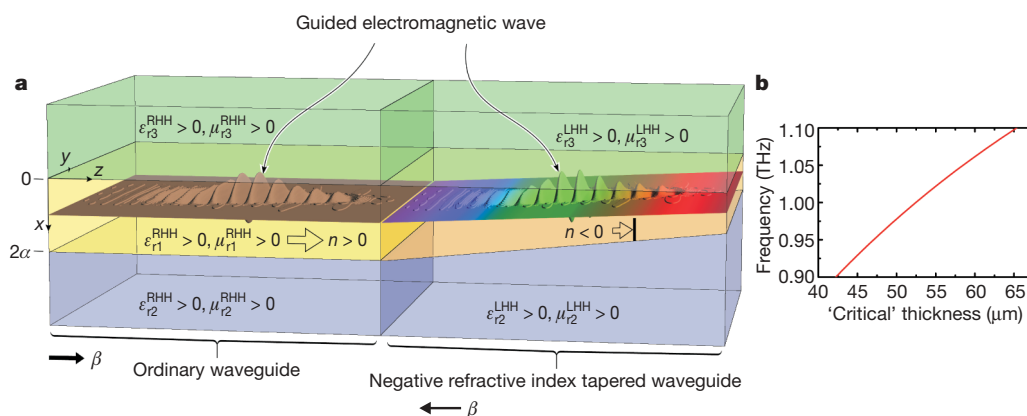


Figure 1 | Trapped rainbow. Different frequency components of a guided wave packet stop at correspondingly different thicknesses inside a tapered left-handed heterostructure (LHH). **a**, The thick open arrows reveal the direction of power flow propagation (P_{tot}^+), while the thin black arrows show the direction of phase propagation (β). The numbering of the layers follows the magnitude of the corresponding refractive indices—that is, in both heterostructures, the middle layer (1) has the highest magnitude of refractive index, followed by the lower layer (2) and, last, by the upper layer (3). A guided wave packet is efficiently injected from the ordinary waveguide to the LHH (see also Fig. 4), inside which it propagates smoothly owing to the slow (adiabatic) reduction in the thickness of the core. The smallest (red) frequency components of the wave are stopped at the smallest core thicknesses of the LHH, while the largest (blue) components stop at correspondingly larger core thicknesses. Thereby, the spectrum of the oscillatory field will be spatially decomposed into its frequency constituents.

After it is trapped, a light ray can be released by locally tuning in real-time the microphotonic structure^{4,9,30} to perturb the repeating 'optical clepsydra' pattern of the ray (Fig 3b–e), and by reversely adiabatically tapering the LHH back to the wide thickness point, which can be impedance-matched to an out-coupling RHH (see Fig. 4). The path of the forward propagating ray inside the reversely tapered LHH (RT-LHH) will be the mirror image of a corresponding backwards propagating ray inside the depicted LHH. From the law of reversibility of the light rays, one then sees that the forward propagating ray inside the RT-LHH, after it has traced its dual path, will reach the wide-thickness end of the structure and will enter the out-coupling RHH with minimal reflection, just as light was initially injected from the in-coupling RHH to our tapered LHH. **b**, An example of the dependence of the 'critical' thicknesses of the LHH on the spectrum of the wave packet. The optogeometric parameters used in this example are those of Fig. 2.

¹Advanced Technology Institute and Department of Physics, Faculty of Engineering and Physical Sciences, University of Surrey, Guildford GU7 1QR, UK. ²Photonics and Nonlinear Science Group, Joule Laboratory, Department of Physics, University of Salford, Salford M5 4WT, UK.

optical amplifiers⁸, photonic crystals^{9,15}, coherent population oscillations¹⁰, stimulated Brillouin scattering¹¹ and surface plasmon polaritons^{12,13} in metalodielectric waveguides have been proposed as means of producing ‘slow light’. However, so far most of these methods bear inherent limitations that may hinder their practical deployment. For instance, electromagnetically induced transparency uses ultracold atomic gases and not solid state materials, quantum-dot semiconductor optical amplifiers usually allow for only modest delays (but for potentially ultra-broadband light pulses), coherent population oscillations and stimulated Brillouin scattering are very narrowband owing to the narrow transparency window of the former and the narrow Brillouin gain bandwidth (around 30 MHz in standard single-mode optical fibres) of the latter, and surface plasmon polaritons are very sensitive to surface roughness and are relatively difficult to excite. Photonic crystals are normally highly multimodal¹⁵; this, combined with the strong impedance mismatch in the ‘slow-light regime’, makes it overly difficult to launch the incoming light energy to a single, slow mode alone¹⁶.

During the same period and in parallel with the above advances, a different, wide-ranging realm of contemporary research has also been developing. It largely followed from a sequence of works by Pendry, Smith and co-workers, in which they proposed practical means for realizing negative refractive index metamaterials¹⁷ and meticulously demonstrated their operation¹⁸. These materials offer a new perspective to the optical world and provide additional degrees of freedom in the design of photonic devices⁵, thereby allowing unprecedented control over the flow of light. A ‘perfect’ lens³, highly anisotropic electromagnetic ‘cloaks’ that render objects invisible to incident

radiation⁶, as well as focusing of electron de Broglie waves by sharp p–n junctions in graphene¹⁹, are a few characteristic examples. Moreover, there is now compelling evidence that, by building on familiar transmission-line concepts borrowed from microwave analysis, such materials can be designed to exhibit broadband negative-index behaviour and relative robustness to losses, all through the microwave region and up to the ultraviolet^{20,21} domain.

In this work, we bring together the realms of metamaterials and slow light as a result of studying the physics associated with wave propagation in slowly, spatially varying negative-index heterostructures. To gain an insight into the physics of the problem at hand, let us for a moment imagine a ray of light propagating in a zigzag fashion along a waveguide with a negative-index (‘left-handed’) core. The ray experiences negative Goos-Hänchen lateral displacements²² each time it strikes the interfaces of the core with the positive-index (‘right-handed’) claddings. Accordingly, the cross points of the incident and reflected rays will sit inside the left-handed core and the effective thickness of the guide will be smaller than its natural thickness (see below). It is reasonable to expect that by gradually reducing the core physical thickness, the effective thickness of the guide will eventually vanish. Obviously, beyond that point the ray will not be able to propagate further down, and will effectively be trapped inside the left-handed heterostructure (LHH). For non-radiative trapping of the ray, we hope that the point where the effective thickness vanishes will not occur below the lower cut-off frequency of the guide. If this condition is fulfilled, then one of the frequencies of a guided wave packet will be completely arrested. The arresting points for the other frequency components will be continuously spaced out. Thereby, one

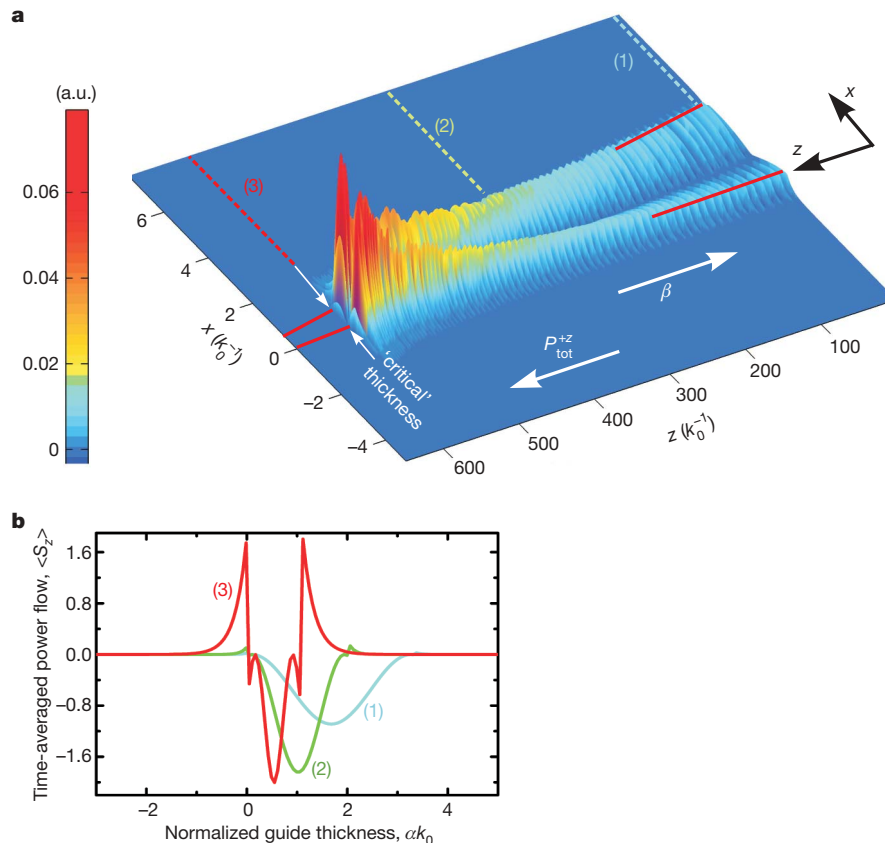


Figure 2 | Wave propagation in an axially varying LHH. The optical parameters of the structure are $\epsilon_{r1}^{\text{LHH}} = -5$, $\epsilon_{r2}^{\text{LHH}} = 2.56$, $\epsilon_{r3}^{\text{LHH}} = 2.25$, $\mu_{r1}^{\text{LHH}} = -5$ and $\mu_{r2}^{\text{LHH}} = \mu_{r3}^{\text{LHH}} = 1$. **a**, A snapshot of the propagation of the monochromatic ($f = 1$ THz) p-polarized magnetic-field component, which enters the LHH from the wide-thickness end ($\alpha k_0 = 1.7$) and stops at the pre-arranged ‘critical’ thickness of $\alpha k_0 \approx 0.55$. The light signal carries a total power $P_{\text{tot}}^{\text{con}} = 82.6 \mu\text{W m}^{-2} \text{s}^{-1}$, which to an excellent approximation is

assumed to be unaffected by the negligibly small reflections from the approaching media interfaces. The group velocity of the wave is parallel to the total power flow P_{tot}^{+z} , while the phase velocity is parallel to the longitudinal propagation constant β . **b**, The evolution of the (discontinuous) time-averaged power flow^{24,26} $\langle S_z \rangle = [\beta / (2\omega\epsilon_0\epsilon_i)] \times |H_y|^2$ from the wide-thickness end (blue line) to the ‘critical’ thickness (red line).

will in principle have a means of stopping light in its tracks and storing it indefinitely, without radiation, over a whole range of frequencies. Such an approach will also be totally immune to atomic decoherence effects²³ and will not require atomic media or group index resonances.

In the following, we show that efficient, broadband, non-radiative storage of light can be realized inside an LHH. We consider an axially non-uniform, linearly tapered, planar waveguide with a core of isotropic and homogeneous negative-index metamaterial, bounded asymmetrically by two positive-index media, as illustrated in Fig. 1a. The simultaneous negativeness of the permittivity ϵ and permeability μ in the left-handed core allows for the existence of efficiently excitable (oscillatory) waveguide modes²⁴, which are not supported by single-negative plasmonic structures. We arrange the variation of the core half-thickness α with distance z to be appropriately slow²⁵ (adiabatic), $d\alpha/dz < 0.05 \times \min\{\alpha k_0 \times (n_{\text{eff},2} - n_{\text{eff},3})/(2\pi)\}$, with αk_0 being the reduced guide thickness, k_0 the free space wavenumber and $n_{\text{eff},2}$, $n_{\text{eff},3}$ the effective indices of the second- and third-order oscillatory modes²⁴, so that the power of a local mode is conserved along the structure. One may then analytically show (see Supplementary Information) that the

electromagnetic fields at a position z_t are given by:

$$\mathbf{G}(x, y, z_t, t) = F(z_t) \mathbf{g}(x, y, \beta(z_t)) \exp \left[i \sum_{z=0}^{z=z_t} \beta(z) \Delta z - i \omega t \right] \quad (1)$$

Here, $\mathbf{G} = \mathbf{E}$ or \mathbf{H} , \mathbf{g} is the solution to the E - or H -field vector wave equation for $z = z_p$, β is the longitudinal propagation constant, ω is the wave angular frequency and F is an appropriate factor, which carries all the information about the mode energy conservation and is calculated as:

$$F = 2\sigma_\epsilon U \left[\frac{\omega \epsilon_0 |\epsilon_{r1}| P_{\text{tot}}^{\text{con}}}{\alpha \beta (W_3^2 + \sigma_\epsilon^2 U^2) \Theta} \right]^{1/2} \quad (2)$$

where $\sigma_\epsilon = \epsilon_{r3}/|\epsilon_{r1}|$, ϵ_{r3} and ϵ_{r1} are the relative permittivities of the upper (3) and middle (1) layers, respectively, $U = \alpha \kappa$ and $W_3 = \alpha \gamma_3$ are the reduced transverse and upper-layer decay constants, respectively (κ and γ_3 are the corresponding unnormalized constants), $P_{\text{tot}}^{\text{con}} = |P_1| + |P_2| + |P_3|$ is the conserved total time-averaged power flow, with P_i ($i = 1, 2, 3$) being the time-averaged power flow in layer i , propagating in the increasing z direction, and:

$$\Theta = 2 + \frac{\rho_\epsilon}{W_2} \frac{U^2 - W_2^2}{W_2^2 + \rho_\epsilon^2 U^2} + \frac{\sigma_\epsilon}{W_3} \frac{U^2 - W_3^2}{W_3^2 + \sigma_\epsilon^2 U^2} \quad (3)$$

with $\rho_\epsilon = \epsilon_{r2}/|\epsilon_{r1}|$ and $W_2 = \alpha \gamma_2$ being the reduced decay constant in the lower layer (γ_2 is the corresponding unnormalized decay constant for the lower layer).

One can judiciously choose the optical parameters of the LHH to facilitate total suppression of all surface polariton modes—that is, the minimum thickness of the core layer can be chosen to be above the upper cut-off of the parasitic surface polariton mode, so that only oscillatory guided modes may exist²⁶. For such a structure, Fig. 1b illustrates an example of ‘critical’ guide thicknesses within which a wave packet, having a spectrum centred at 1 THz, can be completely stopped. Further, Fig. 2 furnishes *ab initio* calculations, following the previously outlined methodology, of the propagating, monochromatic, p-polarized magnetic-field component at a time instant $t = 0$. We find that the

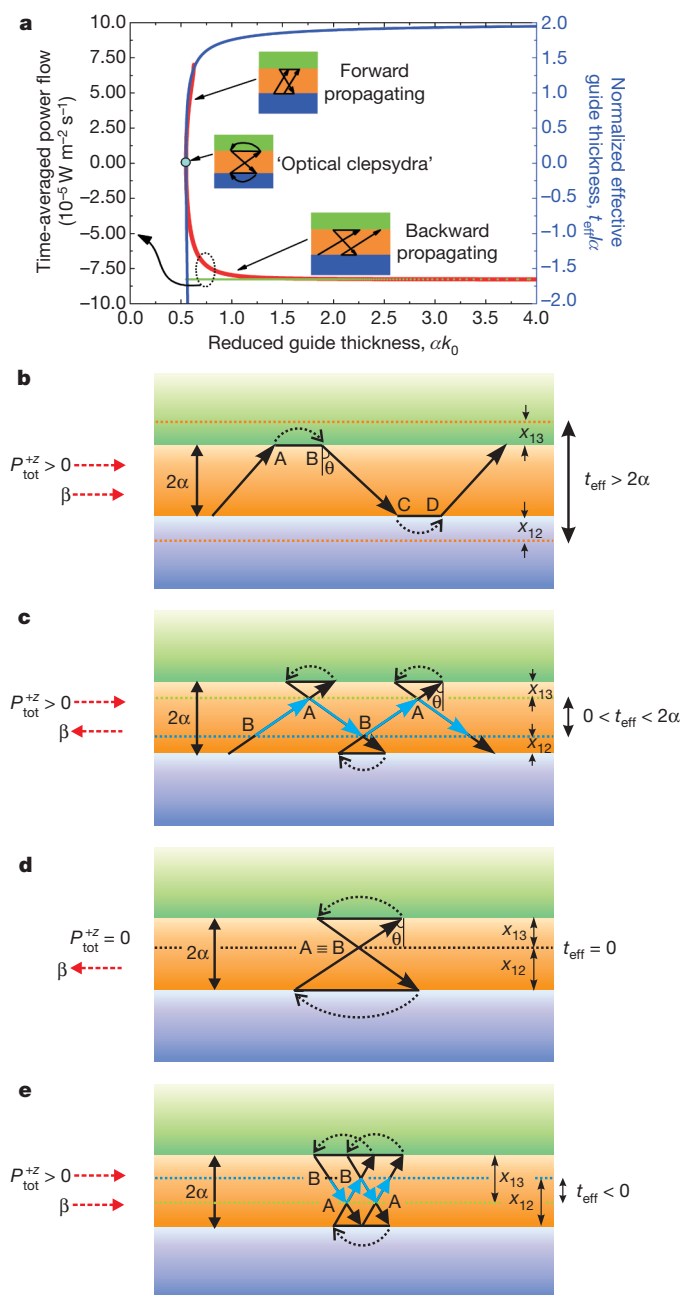


Figure 3 | Ray analysis reveals that the effective left-handed guide thickness is smaller than the physical thickness and can become zero or even negative. **a**, Variations of normalized effective guide thickness t_{eff}/α (solid blue line), conserved $-P_{\text{tot}}^{\text{con}}$ (dotted green line) and forward P_{tot}^{+z} (solid red line) total time-averaged power flow with the reduced guide thickness αk_0 . The forward component (red) of the conserved power flow (green) gradually decreases in magnitude, until it becomes exactly zero at the critical core thickness. At this point, the effective thickness of the LHH also vanishes. For larger guide thicknesses, t_{eff}/α tends asymptotically to the value of 2. The insets associate characteristic regions of P_{tot}^{+z} with the ray analysis results shown in **c–e**. In **b–e**, a ray of light (black), which here signifies power propagation, hits the media interfaces with an angle θ while propagating down the waveguide, and experiences a Goos-Hänchen lateral displacement. The black dotted arrows denote the evanescent field power flow from the optically denser core to the rarer claddings²⁵. In a normal dielectric waveguide^{25,28} (**b**), the Goos-Hänchen phase shifts are positive, the core appears to extend (dotted orange lines) inside the cladding layers and the effective guide thickness is always larger than the physical core thickness 2α . In the slowly varying LHH case (**c–e**), the thickness of the core remains practically constant over many ray periods owing to the slow variation criterion. Here, the ray experiences a negative, that is antiparallel to P_{tot}^{+z} , later displacement originating from the reversed power flow from the core to the claddings and the associated negative Goos-Hänchen phase shift. The two cladding layers now appear to extend inside the core layer (dotted blue and dotted green lines in **c, e**). In **c**, the shifts are relatively small, such that $x_{12} + x_{13} < 2\alpha$. Accordingly, the ray (blue) is effectively confined in the middle region of thickness t_{eff} , by repeatedly bouncing off points A and B. For an appropriate choice of optogeometric parameters (**d**), the two phase shifts can become such that $x_{12} + x_{13} = 2\alpha$ exactly. In this case, t_{eff} vanishes and the ray becomes permanently trapped, forming a double light cone (‘optical clepsydra’). For even larger, compared to the ray period, later displacements (**e**), t_{eff} becomes negative; the ray is still guided in the middle region of thickness $|t_{\text{eff}}|$, but now is forward-propagating, that is, the direction of phase propagation is parallel to the direction of power flow.

magnitude of the total time-averaged power flow propagating in the positive $+z$ direction, $P_{\text{tot}}^{+z} = 1/2 \int_{-\infty}^{\infty} \text{Re}(\mathbf{E} \times \mathbf{H}^*) \cdot \mathbf{z} \, dx$, gradually drops off until it totally peters out (Figs 2b and 3a), even though $P_{\text{tot}}^{\text{con}}$ is conserved along the non-uniform waveguide. Accordingly, one discovers that while the guided oscillatory fields propagate along the structure, with their phase (v_{ph}) and group (v_{g}) velocities being antiparallel, the group and energy (v_{e}) velocities²⁷ progressively decrease, eventually becoming zero at a ‘critical’, pre-determined, guide thickness. At this point, the fields are slowly spatially compressed and amassed²³, with their total amplitude increasing by a factor of 4 for the present set of optogeometric parameters. The exponentially decaying extension of the field inside the lower positive-index layer (medium 3) also progressively increases, as anticipated. Note that in a normal dielectric waveguide the monochromatic oscillatory field would have been reflected and radiated off at the guide cut-off thickness. In that case, an increase in the total amplitude of the field would have been the result of interference between the two light waves propagating in opposite directions. In the present LHH case, however, the wave travels solely in the positive z direction and completely stops upon reaching the ‘critical’ guide thickness; hence, neither reflection nor radiation or interference occur.

The trapping of light is more intuitively recognized by tracing the trajectory of a light ray inside the core for guide thicknesses nearly equal to the critical one mentioned above (see Fig. 3). Recall that the variation of the core refractive index with distance z is much smaller than the ray half-period z_{hp} , so that locally the guide appears practically uniform. Let us assume that the light ray arrives at the 1–3 media interface of the LHH with an angle θ (Fig. 3c–e). Following reflection from this interface, the ray experiences a Goos-Hänchen phase shift²² $\delta_{p13} = -2 \tan^{-1} [W_3/(\sigma_e U)]$, which is equal in magnitude but opposite in sign to the shift of the corresponding positive-index case. Detailed calculations then reveal that the distance x_{p13} between the cross point A of the two rays (Fig. 3c–e) and the 1–3 media interface is (see Supplementary Information) $x_{p13} = (\alpha \sigma_e V_3^2) / [W_3(W_3^2 + \sigma_e^2 U^2)]$, where $V_3^2 = U^2 + W_3^2$. Likewise, the distance x_{p12} between point B and the 1–2 interface is $x_{p12} = (\alpha \rho_e V_2^2) / [W_2(W_2^2 + \rho_e^2 U^2)]$, where $V_2^2 = U^2 + W_2^2$. One is, thus, led to discern (Fig. 3c, blue line) that the light ray is effectively altogether confined within the middle region of thickness t_{eff} wherein it repeatedly bounces off points A and B.

We argue that $t_{\text{eff}} = 2\alpha - x_{p12} - x_{p13}$ is the effective thickness of the left-handed waveguiding heterostructure. This conclusion is strongly supported by the preceding remarks concerning the ray trajectory, and can be formally established by noting that the total time-averaged power flow P_{tot}^{+z} can be directly linked to t_{eff} through the following relation (see Supplementary Information):

$$P_{\text{tot}}^{+z} = \frac{1}{4} E_x^{\text{max}} H_y^{\text{max}} t_{\text{eff}} \quad (4)$$

where E_x^{max} and H_y^{max} are the maximum values of the E_x - and H_y -field components in the guide, respectively. The similarities between equation (4) and its counterpart in the case of conventional, right-handed heterostructures (RHH)²⁸, allow one to conclusively infer that t_{eff} , as defined in equation (4) is, indeed, the effective thickness of the LHH. However, in stark contrast to conventional waveguides, t_{eff} is here always smaller than the physical thickness of the core, and can become zero (Fig. 3d) or even negative (Fig. 3e). When t_{eff} becomes negative, we deduce from equation (4) that P_{tot}^{+z} and β become parallel; thereby, the corresponding guided mode will be a forward-propagating one. Interestingly, on the basis of Fig. 3a and equation (4) we infer that for a particular value of the guide’s physical thickness 2α , the effective thickness vanishes. In this case, the lateral shifts x_{p12} , x_{p13} experienced by the ray upon reflection from the two interfaces are such that $x_{p12} + x_{p13} = 2\alpha$ exactly. For the aforementioned ‘critical’ physical thickness, the light ray is permanently trapped inside the LHH, being unable to propagate further down. From Fig. 3d we see that in this case the trajectory of the ray forms a double light-cone. In view of its characteristic hourglass form, we will call it the ‘optical clepsydra’.

Following a similar course of analysis, we discover that for different excitation frequencies the guided oscillatory fields stop at correspondingly different guide thicknesses. Accordingly, a guided electromagnetic wave packet can be altogether trapped within a fixed area, spanning a continuous range of guide thicknesses. The leading (trailing) part of the pulse, composed of the smallest (highest) frequencies (Fig. 3a), stops at the smallest (highest) guide thicknesses. Thereby, in the small-intensity, linear case—in which the propagating spectral power densities of a ‘white’ wave packet do not couple⁸, and the guided field is a linear, weighted sum of its single frequency constituents—the ‘red’ and ‘blue’ components of the field will be spatially separated (Fig. 1). This is similar to the separation of the colours of the visible spectrum and the appearance of a rainbow when sunlight illuminates a transparent prism or falling water droplets. For this reason, we shall henceforth call the stopping and storing of light in such LHHs the ‘trapped rainbow’ effect.

A critical characteristic of the axially varying LHH is that further away from the point where the trapping of the light beam is arranged to occur (that is, for larger guide thicknesses) it is possible to achieve complete impedance matching with a dielectric waveguide. We recall that for waveguide structures, the characteristic impedance is defined as $Z_0^{PV} = (V_0 V_0^*) / (2P_{\text{tot}}^{+z})$, where V_0 is a ‘voltage’ defined as the line integral of the electric field along some path, which starts from below the lower interface and ends amply above the upper one²⁹. Figure 4 illustrates the variation with reduced guide thickness of the analytically calculated (see Supplementary Information) ordinary and left-handed waveguide characteristic impedances. At a point sufficiently far from the ‘critical’ thickness of the LHH, its characteristic impedance becomes equal to that of a normal waveguide. At this point ($\sim 12.76 \alpha k_0$ in our case) the two structures also have equal thicknesses. Moreover, the spatial distribution of the guided field at the wide end of the LHH (Fig. 4 inset, red line) closely matches the field distribution of a single-mode optical waveguide. Accordingly, a light wave launched from a dielectric guide to a wide-thickness LHH will experience minimal reflection, mainly owing to minute mode-mismatch, which can be further adjusted and optimized at will.

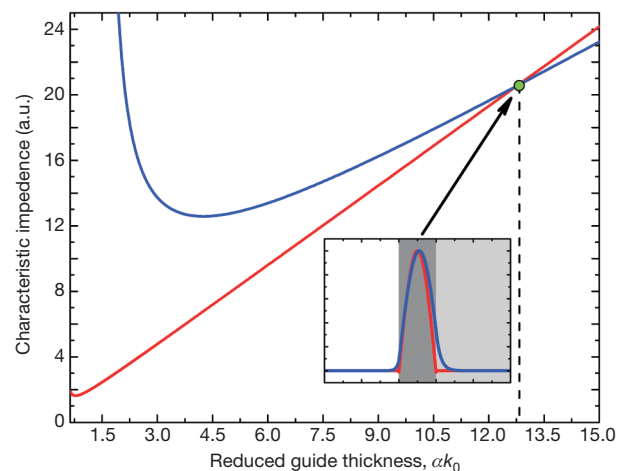


Figure 4 | Honed conditions for waveguide coupling, showing simultaneous impedance, thickness and mode matching in adjoining RHH and LHHs. The optical parameters of the LHH are similar to those in Fig. 2. For the RHH we have $\epsilon_{r1}^{\text{RHH}} = 1.5625$, $\epsilon_{r2}^{\text{RHH}} = 1.44$, $\epsilon_{r3}^{\text{RHH}} = 1.21$, $\mu_{r1}^{\text{RHH}} = \mu_{r2}^{\text{RHH}} = \mu_{r3}^{\text{RHH}} = 1$. The characteristic impedance of the dielectric waveguide (blue) exhibits a dip at $\alpha k_0 \approx 4.53$, after which it grows monotonically. A similar trend is found for the characteristic impedance of the LHH (red). Here, the minimum value occurs at a guide thickness $\alpha k_0 \approx 0.89$ and at the ‘critical’ LHH thickness it diverges. The two curves cross at $\alpha k_0 \approx 12.77$. The inset shows the profile of the fundamental (blue) and second-order oscillatory²⁴ (red) mode of the dielectric waveguide and LHH, respectively, at the cross point. The darker the shaded region in the inset, the higher is the magnitude of the refractive index.

In summary, we have shown how guided electromagnetic fields can be brought efficiently to a complete standstill while travelling inside axially varying left-handed waveguiding heterostructures. The scheme invokes solid-state materials and, as such, is not subject to low-temperature or atomic coherence limitations. Moreover, it inherently allows for high in-coupling efficiencies and broadband function, as the deceleration of light does not rely on refractive index resonances. This ‘trapped rainbow’ method for storing photons opens the way to a multitude of hybrid, optoelectronic devices to be used in ‘quantum information’ processing, communication networks and signal processors, and could lead to combined metamaterials and slow-light research.

Received 5 July; accepted 19 September 2007.

- Born, M. & Wolf, E. *Principles of Optics* 6th edn (Pergamon, Oxford, 1980).
- Grigorenko, A. N. *et al.* Nanofabricated media with negative permeability at visible frequencies. *Nature* **438**, 335–338 (2005).
- Pendry, J. B. Negative refraction makes a perfect lens. *Phys. Rev. Lett.* **85**, 3966–3969 (2000).
- Hou-Tong, C. *et al.* Active terahertz metamaterial devices. *Nature* **444**, 597–600 (2006).
- Pendry, J. B., Schurig, D. & Smith, D. R. Controlling electromagnetic fields. *Science* **312**, 1780–1782 (2006).
- Schurig, D. *et al.* Metamaterial electromagnetic cloak at microwave frequencies. *Science* **314**, 977–980 (2006).
- Liu, C., Dutton, Z., Behroozi, C. H. & Hau, L. V. Observation of coherent optical information storage in an atomic medium using halted light pulses. *Nature* **409**, 490–493 (2001).
- Gehrig, E., van der Poel, M., Mørk, J. & Hess, O. Dynamic spatiotemporal speed control of ultrashort pulses in quantum-dot SOAs. *IEEE J. Quant. Electron.* **42**, 1047–1054 (2006).
- Vlasov, Y. A., O’Boyle, M., Hamann, H. F. & McNab, S. J. Active control of slow light on a chip with photonic crystal waveguides. *Nature* **438**, 65–69 (2005).
- Bigelow, M. S., Lepeshkin, N. N. & Boyd, R. W. Superluminal and slow light propagation in a room-temperature solid. *Science* **301**, 200–202 (2003).
- Okawachi, Y. *et al.* Tunable all-optical delays via Brillouin slow light in an optical fiber. *Phys. Rev. Lett.* **94**, 153902 (2005).
- Stockman, M. I. Nanofocusing of optical energy in tapered plasmonic waveguides. *Phys. Rev. Lett.* **93**, 137404 (2004).
- Karalis, A., Lidorikis, E., Ibanescu, M., Joannopoulos, J. D. & Soljačić, M. Surface-plasmon-assisted guiding of broadband slow and subwavelength light in air. *Phys. Rev. Lett.* **95**, 063901 (2005).
- Blumenthal, D. J., Prunçal, P. R. & Sauer, J. R. Photonic packet switches: Architectures and experimental implementations. *Proc. IEEE* **82**, 1650–1667 (1994).
- Gersen, H. *et al.* Real-space observation of ultraslow light in photonic crystal waveguides. *Phys. Rev. Lett.* **94**, 073903 (2005).
- Vlasov, Y. A. & McNab, S. J. Coupling into the slow light mode in slab-type photonic crystal waveguides. *Opt. Lett.* **31**, 50–52 (2006).
- Pendry, J. B., Holden, A. J., Robbins, D. J. & Stewart, W. J. Magnetism from conductors and enhanced nonlinear phenomena. *IEEE Trans. Microwave Theory Tech.* **47**, 2075–2084 (1999).
- Shelby, R., Smith, D. R. & Schultz, S. Experimental verification of a negative index of refraction. *Science* **292**, 77–79 (2001).
- Cheianov, V. V., Fal’ko, V. & Altshuler, B. L. The focusing of electron flow and a Veselago lens in graphene p-n junctions. *Science* **315**, 1252–1255 (2007).
- Shalaev, V. M. Optical negative-index metamaterials. *Nature Photonics* **1**, 41–48 (2007).
- Alù, A. & Engheta, N. Three-dimensional nanotransmission lines at optical frequencies: A recipe for broadband negative-refraction optical metamaterials. *Phys. Rev. B* **75**, 024304 (2007).
- Berman, P. R. Goos-Hänchen shift in negatively refractive media. *Phys. Rev. E* **66**, 067603 (2002).
- Milonni, P. W. *Fast Light, Slow Light and Left-Handed Light* Chs 5–6 (Institute of Physics, Bristol, 2005).
- Tsakmakidis, K. L., Klaedtke, A., Aryal, D. P., Jamois, C. & Hess, O. Single-mode operation in the slow-light regime using oscillatory waves in generalized left-handed heterostructures. *Appl. Phys. Lett.* **89**, 201103 (2006).
- Snyder, A. & Love, J. D. *Optical Waveguide Theory* Chs 5–19 (Chapman and Hall, New York, 1983).
- Tsakmakidis, K. L., Hermann, C., Klaedtke, A., Jamois, C. & Hess, O. Surface plasmon polaritons in generalized slab heterostructures with negative permittivity and permeability. *Phys. Rev. B* **73**, 085104 (2006).
- Boardman, A. D. & Marinov, K. Electromagnetic energy in a dispersive metamaterial. *Phys. Rev. B* **73**, 165110 (2006).
- Tamir, T. (ed.) *Integrated Optics* Ch. 2 (Springer, New York, 1979).
- Helszajn, J. *Ridge Waveguides and Passive Microwave Components* (IEE Press, London, 2000).
- Povinelli, M. L. *et al.* Evanescent-wave bonding between optical waveguides. *Opt. Lett.* **30**, 3042–3044 (2005).

Supplementary Information is linked to the online version of the paper at www.nature.com/nature.

Acknowledgements We thank A. Klaedtke and D. P. Aryal for discussions and technical assistance. This work was supported by the Engineering and Physical Sciences Research Council (UK).

Author Contributions K.L.T. and O.H. conceived the presented idea. K.L.T. developed the theory, performed the computations and wrote a draft of the paper. A.D.B. contributed to the discussions. O.H. encouraged K.L.T. to investigate metamaterials and slow light and supervised the findings of the work.

Author Information Reprints and permissions information is available at www.nature.com/reprints. Correspondence and requests for materials should be addressed to K.L.T. (K.Tsakmakidis@surrey.ac.uk) or O.H. (O.Hess@surrey.ac.uk).